

N-ORDER BRIGHT AND DARK ROGUE WAVES IN A RESONANT ERBIUM-DOPED FIBRE SYSTEM

Jingsong He ^{a*}, *Shuwei Xu* ^b and *K. Porseizan* ^c

^a Department of Mathematics, Ningbo University, Ningbo, Zhejiang 315211, P.R. China

^b School of Mathematical Sciences, USTC, Hefei, Anhui 230026, P.R. China

^c Department of Physics, Pondicherry University, Puducherry 605014, India

ABSTRACT. The rogue waves in a resonant erbium-doped fibre system governed by a coupled system of the nonlinear Schrödinger equation and the Maxwell-Bloch equation (NLS-MB equations) are given explicitly by a Taylor series expansion about the breather solutions of the normalized slowly varying amplitude of the complex field envelope E , polarization p and population inversion η . The n-order breather solutions of the three fields are constructed using Darboux transformation (DT) by assuming periodic seed solutions. What is more, the n-order rogue waves are given by determinant forms with $n+3$ free parameters. Furthermore, the possible connection between our rogue waves and the generation of supercontinuum generation is discussed.

Key words: NLS-MB equations, Darboux transformation, breather solutions, rogue waves, dark rogue waves.

PACS numbers: 02.30.Ik, 42.81.Dp, 52.35.Bj, 52.35.Sb, 94.05.Fg

1. INTRODUCTION

In recent years, long haul optical communication through fibers has attracted considerable interest in research activities among scientists all over the world. Especially, it has been demonstrated that the soliton-type pulse propagation will play a vital role in the ultra fast communication systems. They are considered to be the futuristic tools in achieving low-loss, cost-effective high speed communication throughout the world. Soliton-type pulse propagation through nonlinear optical fibers is realized by means of the exact counterbalance between the major constraints of the fiber, viz., group velocity dispersion (linear effect) which broadens the pulse and the self-phase modulation (nonlinear effect) which contracts the pulse. The propagation of optical pulses through a nonlinear fiber in the picosecond regime is described by the well-known nonlinear Schrödinger (NLS) equation, which was first proposed by Hasegawa and Tappert in 1973 [1].

To make the soliton based communication systems highly competitive, reliable and economical when compared to the conventional systems, attenuation in a fiber must be compensated. A different type of optical soliton is associated with the self-induced transparency (SIT) effect in resonant absorbers. The soliton pulse propagation in an erbium doped fiber amplifier utilizes the SIT phenomena, first discovered by McCall and Hahn [2]. In 1967, McCall and Hahn proposed a new type of optical soliton in a two level resonant system. Above a well-defined threshold intensity, short resonant pulses of a given duration will propagate through a normally absorbing medium with anomalously low attenuation. This happens when the pulse width is short, compared to the relaxation times in the medium and the pulse centre frequency is in resonance with a two-level absorbing transition. After a few classical absorption lengths, the pulse achieves a steady state in which its width, energy and shape remain constant. The pulse velocity has greatly reduced from the normal velocity of light in such media. With these properties, the pulse propagation of this type is named "self-induced transparency" (SIT) soliton and frequently described by the Maxwell-Bloch (MB) equations. They are

$$\begin{aligned} E_z &= p, \\ p_t &= i \omega_0 p - f q \eta, \end{aligned}$$

* Corresponding author: hejingsong@nbu.edu.cn, jshe@ustc.edu.cn.

$$\eta_t = f(qp^* + q^*p), \quad (1)$$

Here, E and p are complex variables, η is a real variable and ω_0 is a real constant and f is the character describing the interaction between the resonant atoms and the optical field. The symbol $*$ denotes the complex conjugate. These equations can be extended to the case of fiber amplifiers. When Er is doped with the core of the optical fibres, then the nonlinear wave propagation can have both the effects due to silica and Er impurities. Er impurities give SIT effect to the optical pulse, whereas the silica material gives the NLS soliton effect. So if we consider these effects for a large width pulse, then the system dynamics will be governed by the coupled system of the NLS equation and the MB equation (NLS-MB system). Maimistov et al [3], in 1983 proposed the system and obtained the Lax pair and the inverse scattering transform technique for the soliton solution. The NLS-MB equations read as [3]

$$\begin{aligned} E_t &= i\left[\frac{1}{2}E_{xx} + |E|^2 E\right] + 2p, \\ p_x &= 2i\omega_0 p + 2E\eta, \\ \eta_x &= -(Ep^* + E^*p), \end{aligned} \quad (2)$$

The above equation have also been reduced through the Painleve analysis [4]. Further, Kakei and Satsuma [5] also reported the Lax pair and the multi-soliton solution of the NLS-MB equations. The integrability aspects of NLS-MB system with variable dispersion, the study of propagation of optical solitons in coupled NLS-MB, and random nonuniform-doped media have been reported earlier wherein the spectral parameter was kept constant. The coexistence of NLS soliton and SIT soliton has already been confirmed experimentally. The propagation and switching of SIT in nonlinear directional couplers with two-level atom nonlinearity has been recently investigated numerically by retaining the transverse dependence of the optical field and atomic variable. Recent experiments by Nakazawa *et al.*, have confirmed guided wave SIT soliton formation and propagation by employing a few meters of erbium doped fibre [6, 7].

Recently, considering all higher order effects in the propagation of femtosecond pulses, the coupled Hirota and Maxwell-Bloch (CH-MB) equations have been proposed and analyzed for soliton solutions [8]. Some generalization of NLS-MB equations, for instance, the CH-MB equations and the NLS-MB equations with variable dispersion and nonlinear effects are discussed [9–11]. The single soliton and the single breather solutions [12] of the NLS-MB equations are given by the Darboux transformation (DT) [13, 14].

In recent years, in addition to solitons in different optical systems, the study of rogue waves have also attracted considerable interest because of their potential applications in different branches of physics including oceanography [15–18], which occurs due to either modulation instability [19–25], or random initial condition [18, 26]. The first order rogue wave is most likely to appear as a single peak hump with two caves in a plane with a nonzero boundary. One of the possible generating mechanisms for rogue waves is the creation of breathers which can be realized by modulation instability. Then, larger rogue waves can build up when two or more breathers collide themselves [27–33]. Recently, more general higher-order rogue waves were obtained such as showing that these general N -th order rogue waves contain $N - 1$ free irreducible complex parameters [31]. Rogue waves can also be observed in space plasmas [34–39] and optics when propagating high power optical radiation through photonic crystal fibers [40–42]. Considering all higher order effects in the propagation of femtosecond pulses, rogue waves can also be observed in a system modeled by the Hirota equation [43–45]. Furthermore, rogue waves have not only been observed in continuous media but have also been reported in discrete systems, such as the systems of the well-known Ablowitz-Ladik (A-L) equation [46].

Though the rogue waves have been reported in different branches of physics where the system dynamics is governed by single equation, to the best our knowledge, they have been observed and reported very little in the coupled systems. For example, Rogue waves of the coupled NLS were

constructed in the literatures [47–49]. Very recently, new kinds of matter rogue waves [50] have been reported in $F = 1$ spinor Bose-Einstein condensate system controlled by three component NLS equation. In experiment, the rogue waves in a multistable system [51] is revealed by experiments with an erbium-doped fiber laser driven by harmonic pump modulation. So, it is our prime interest to analyze the possibility of rogue waves in coupled systems, such as NLS-MB system.

It is well known that the dark soliton [52] of the defocusing nonlinear Schrödinger (NLS) equation is essentially different from that of bright soliton. For the past two decades or so, intensive research have been carried by several groups about theoretical and experimental aspects of dark bright solitons, it is quite natural to ask a question: is there any possibility of observing dark rogue wave in soliton equations? In general, the first order dark rogue wave has one down dominant peak and two small lumps. Because of the singularity [13, 14] of the solution for the de-focusing NLS equation generated by using DT, we cannot get dark rogue wave of the de-focusing by this way. Fortunately, we have obtained dark and bright rogue waves [53] of the NLS-MB equations from a Taylor series expansion of the first order breather solutions, which are generated from a periodic seed by the DT. But we did not provide a detailed analysis on their dynamical evolution and higher order rogue waves. The aim of this paper is twofold. Firstly, the determinant representation of the n-fold DT of the NLS-MB equations are similar to the case of NLS equation DT [54]. Secondly, the rogue waves of the three optical fields are constructed by determinant forms. It should be noted that the rogue waves of the fields p and η are dark. Furthermore, the connection between our rogue waves and the generation of supercontinuum generation will be discussed.

The organization of this paper is as follows. In section 2, the determinant representation of the n-fold DT and formulae of $E^{[n]}$, $p^{[n]}$ and $\eta^{[n]}$ are expressed by eigenfunctions of spectral problem. In section 3, a Taylor series expansion about the breather solutions are generated by n-fold DT from a periodic seed solution with a constant amplitude to construct the bright and dark rogue waves. What is more, the n-order rogue waves are given by determinant forms with $n + 3$ free parameters. Finally, we conclude the results in section 4.

2. DARBOUX TRANSFORMATION

The linear spectral problem of the NLS-MB equations can be expressed as [3]

$$\Psi_x = U\Psi, \quad (3)$$

$$\Psi_t = V\Psi, \quad (4)$$

where

$$\begin{aligned} \Psi &= \begin{pmatrix} \Psi_1 \\ \Psi_2 \end{pmatrix}, \\ U &= \begin{bmatrix} \lambda & E \\ -E^* & -\lambda \end{bmatrix} \equiv \lambda\sigma_3 + U_0, \\ V &= i \left(\begin{bmatrix} 1 & 0 \\ 0 & -1 \end{bmatrix} \lambda^2 + \begin{bmatrix} 0 & E \\ -E^* & 0 \end{bmatrix} \lambda + \frac{1}{2} \begin{bmatrix} |E|^2 & E_x \\ E_x^* & -|E|^2 \end{bmatrix} \right) + \frac{1}{\lambda - i \omega_0} \begin{pmatrix} \eta & -p \\ -p^* & -\eta \end{pmatrix} \\ &\equiv i\sigma_3\lambda^2 + i\lambda V_1 + \frac{i}{2}V_0 + \frac{1}{\lambda - i \omega_0}V_{-1}, \end{aligned}$$

and λ is the complex eigenvalue parameter.

It is easy to prove that the spectral problem (3) and (4) are transformed to

$$\Psi^{[1]}_x = U^{[1]} \Psi^{[1]}, \quad U^{[1]} = (T_x + T U)T^{-1}, \quad (5)$$

$$\Psi^{[1]}_t = V^{[1]} \Psi^{[1]}, \quad V^{[1]} = (T_t + T V)T^{-1}, \quad (6)$$

under a gauge transformation

$$\Psi^{[1]} = T \Psi. \quad (7)$$

Here, T is a 2×2 matrix, which is determined by the cross differentiating (5) and (6),

$$U^{[1]}_t - V^{[1]}_x + [U^{[1]}, V^{[1]}] = T(U_t - V_x + [U, V])T^{-1}. \quad (8)$$

This implies that, in order to make eq.(3) and eq.(4) invariant under the transformation (7), it is crucial to search a matrix T such that $U^{[1]}$ and $V^{[1]}$ have the same forms as U and V . At the same time the old potential (or seed solutions) (E, p, η) in spectral matrixes U and V are mapped into new potentials (or new solutions) $(E^{[1]}, p^{[1]}, \eta^{[1]})$ in terms of new spectral matrixes $U^{[1]}$ and $V^{[1]}$.

2.1 One-fold Darboux transformation of NLS-MB equations

In order to be self-contained, we shall recall the one-fold DT [12] of NLS-MB equations. Considering the application of the representation for the n-fold DT by means of the determinant [54] of eigenfunctions with different eigenvalues in the following context, we need to introduce $2n$ eigenfunctions by $f_k = f_k(\lambda_k) = \begin{pmatrix} f_{k1} \\ f_{k2} \end{pmatrix}$ associated with an eigenvalue λ_k , and $\lambda_k = \lambda_m$ if $k = m$, where $k = 1, 2, 3, \dots, 2n$ but $\lambda_k \neq \lambda$. Additionally, the eigenfunctions for distinct eigenvalues are linearly independent, (i.e.) f_k and f_m are linearly independent if $k \neq m$.

The elements of one-fold DT [12] are parameterized by the eigenfunction f_k associated with λ_k as

$$T_1(\lambda; \lambda_1, \lambda_2) = \lambda I + S = \begin{pmatrix} \widetilde{(T_1)_{11}} & \widetilde{(T_1)_{12}} \\ \widetilde{(T_1)_{21}} & \widetilde{(T_1)_{22}} \end{pmatrix}, \quad (9)$$

Here I is a unit matrix, and

$$S = \begin{pmatrix} \frac{\begin{vmatrix} -\lambda_1 f_{11} & f_{12} \\ -\lambda_2 f_{21} & f_{22} \end{vmatrix}}{|W_2|} & \frac{\begin{vmatrix} f_{11} & -\lambda_1 f_{11} \\ f_{21} & -\lambda_2 f_{21} \end{vmatrix}}{|W_2|} \\ \frac{\begin{vmatrix} -\lambda_1 f_{12} & f_{12} \\ -\lambda_2 f_{22} & f_{22} \end{vmatrix}}{|W_2|} & \frac{\begin{vmatrix} f_{11} & -\lambda_1 f_{12} \\ f_{21} & -\lambda_2 f_{22} \end{vmatrix}}{|W_2|} \end{pmatrix},$$

$$W_2(f_1, f_2) = \begin{pmatrix} f_{11} & f_{12} \\ f_{21} & f_{22} \end{pmatrix}, \det(T_1) = (\lambda - \lambda_1)(\lambda - \lambda_2),$$

$$\widetilde{(T_1)_{11}} = \begin{vmatrix} 1 & 0 & \lambda \\ f_{11} & f_{12} & \lambda_1 f_{11} \\ f_{21} & f_{22} & \lambda_2 f_{21} \end{vmatrix}, \widetilde{(T_1)_{12}} = \begin{vmatrix} 0 & 1 & 0 \\ f_{11} & f_{12} & \lambda_1 f_{11} \\ f_{21} & f_{22} & \lambda_2 f_{21} \end{vmatrix},$$

$$\widetilde{(T_1)_{21}} = \begin{vmatrix} 1 & 0 & 0 \\ f_{11} & f_{12} & \lambda_1 f_{12} \\ f_{21} & f_{22} & \lambda_2 f_{22} \end{vmatrix}, \widetilde{(T_1)_{22}} = \begin{vmatrix} 0 & 1 & \lambda \\ f_{11} & f_{12} & \lambda_1 f_{12} \\ f_{21} & f_{22} & \lambda_2 f_{22} \end{vmatrix}.$$

With the transformed potentials,

$$U_0^{[1]} = U_0 - [\sigma_3, T_1],$$

$$V_{-1}^{[1]} = T_1|_{\lambda=i\omega_0} V_{-1} T_1^{-1}|_{\lambda=i\omega_0}, \quad (10)$$

The resulting new solutions of $E^{[1]}$, $p^{[1]}$ and $\eta^{[1]}$ are given by

$$E^{[1]} = E - 2S_{12}, \quad (11)$$

$$p^{[1]} = -\frac{1}{\det(T_1)}(-2\eta(T_1)_{11}(T_1)_{12} + p^*(T_1)_{12}(T_1)_{12} - p(T_1)_{11}(T_1)_{11})|_{\lambda=i\omega_0}, \quad (12)$$

$$\eta^{[1]} = \frac{1}{\det(T_1)}(\eta((T_1)_{11}(T_1)_{22} + (T_1)_{12}(T_1)_{21}) - p^*(T_1)_{12}(T_1)_{22} + p(T_1)_{11}(T_1)_{21})|_{\lambda=i\omega_0}, \quad (13)$$

and the new eigenfunction $f_k^{[1]}$ of λ_k corresponding to the new potentials is

$$f_k^{[1]} = \begin{pmatrix} \begin{vmatrix} f_{k1} & f_{k2} & \lambda_k f_{k1} \\ f_{11} & f_{12} & \lambda_1 f_{11} \\ f_{21} & f_{22} & \lambda_2 f_{21} \end{vmatrix} \\ \hline |W_2| \\ \begin{vmatrix} f_{k1} & f_{k2} & \lambda_k f_{k2} \\ f_{11} & f_{12} & \lambda_1 f_{12} \\ f_{21} & f_{22} & \lambda_2 f_{22} \end{vmatrix} \\ \hline |W_2| \end{pmatrix}.$$

In order to satisfy the constraints of S' and V'_{-1} in [12], set

$$\lambda_2 = -\lambda_1^*, f_2 = \begin{pmatrix} -f_{12}^* \\ f_{11}^* \end{pmatrix}. \quad (14)$$

2.2 n-fold Darboux transformation for NLS-MB equations

In this subsection, our prime aim is to establish the determinant representation of the n-fold DT for NLS-MB equations as we have done for the case of NLS equation [54]. According to the form of T_1 in eq.(9), the n-fold DT should be of the form $T_n = T_n(\lambda) = \lambda^n I + t_1 \lambda^{n-1} + t_2 \lambda^{n-2} + \dots + t_{n-1} \lambda + t_n$, where t_i are 2×2 matrices, $i = 1, 2, \dots, n$. T_n which leads to the determinant representation of T_n by means of its kernel. Specifically, from algebraic equations,

$$f_k^{[n]} = T_n(\lambda; \lambda_1, \lambda_2, \dots, \lambda_{2n-1}, \lambda_{2n})|_{\lambda=\lambda_i} f_k = \sum_{l=0}^n t_l \lambda_k^l f_k = 0, i = 1, 2, \dots, 2n-1, 2n, \quad (15)$$

with

$$t_0 = \begin{pmatrix} 1 & 0 \\ 0 & 1 \end{pmatrix},$$

coefficients t_l , $l = 1, 2, \dots, n$ are solved by Cramer's rule. Thus we obtain the determinant representation of the T_n .

Theorem 1. The n-fold DT of the NLS-MB equations is $T_n = T_n(\lambda) = \lambda^n I + t_1 \lambda^{n-1} + t_2 \lambda^{n-2} + \dots + t_{n-1} \lambda + t_n$, where t_i are 2×2 matrices, $i = 1, 2, \dots, n$. The final form of $T_n(\lambda)$ has the form,

$$T_n = T_n(\lambda; \lambda_1, \lambda_2, \dots, \lambda_{2n-1}, \lambda_{2n}) = \begin{pmatrix} \widetilde{(T_n)_{11}} & \widetilde{(T_n)_{12}} \\ \hline \widetilde{|W_{2n}|} & \widetilde{|W_{2n}|} \\ \widetilde{(T_n)_{21}} & \widetilde{(T_n)_{22}} \\ \hline \widetilde{|W_{2n}|} & \widetilde{|W_{2n}|} \end{pmatrix}, \quad (16)$$

$$\widetilde{(Q_n)_{12}} = - \begin{vmatrix} f_{11} & f_{12} & \lambda_1 f_{11} & \lambda_1 f_{12} & \lambda_1^2 f_{11} & \lambda_1^2 f_{12} & \dots & \lambda_1^{n-1} f_{11} & \lambda_1^n f_{11} \\ f_{21} & f_{22} & \lambda_2 f_{21} & \lambda_2 f_{22} & \lambda_2^2 f_{21} & \lambda_2^2 f_{22} & \dots & \lambda_2^{n-1} f_{21} & \lambda_2^n f_{21} \\ f_{31} & f_{32} & \lambda_3 f_{31} & \lambda_3 f_{32} & \lambda_3^2 f_{31} & \lambda_3^2 f_{32} & \dots & \lambda_3^{n-1} f_{31} & \lambda_3^n f_{31} \\ \vdots & \vdots \\ f_{2n1} & f_{2n2} & \lambda_{2n} f_{2n1} & \lambda_{2n} f_{2n2} & \lambda_{2n}^2 f_{2n1} & \lambda_{2n}^2 f_{2n2} & \dots & \lambda_{2n}^{n-1} f_{2n1} & \lambda_{2n}^n f_{2n1} \end{vmatrix},$$

$$\widetilde{(Q_n)_{21}} = \begin{vmatrix} f_{11} & f_{12} & \lambda_1 f_{11} & \lambda_1 f_{12} & \lambda_1^2 f_{11} & \lambda_1^2 f_{12} & \dots & \lambda_1^{n-1} f_{12} & \lambda_1^n f_{12} \\ f_{21} & f_{22} & \lambda_2 f_{21} & \lambda_2 f_{22} & \lambda_2^2 f_{21} & \lambda_2^2 f_{22} & \dots & \lambda_2^{n-1} f_{22} & \lambda_2^n f_{22} \\ f_{31} & f_{32} & \lambda_3 f_{31} & \lambda_3 f_{32} & \lambda_3^2 f_{31} & \lambda_3^2 f_{32} & \dots & \lambda_3^{n-1} f_{32} & \lambda_3^n f_{32} \\ \vdots & \vdots \\ f_{2n1} & f_{2n2} & \lambda_{2n} f_{2n1} & \lambda_{2n} f_{2n2} & \lambda_{2n}^2 f_{2n1} & \lambda_{2n}^2 f_{2n2} & \dots & \lambda_{2n}^{n-1} f_{2n2} & \lambda_{2n}^n f_{2n2} \end{vmatrix},$$

$$\widetilde{(Q_n)_{22}} = - \begin{vmatrix} f_{11} & f_{12} & \lambda_1 f_{11} & \lambda_1 f_{12} & \lambda_1^2 f_{11} & \lambda_1^2 f_{12} & \dots & \lambda_1^{n-1} f_{11} & \lambda_1^n f_{12} \\ f_{21} & f_{22} & \lambda_2 f_{21} & \lambda_2 f_{22} & \lambda_2^2 f_{21} & \lambda_2^2 f_{22} & \dots & \lambda_2^{n-1} f_{21} & \lambda_2^n f_{22} \\ f_{31} & f_{32} & \lambda_3 f_{31} & \lambda_3 f_{32} & \lambda_3^2 f_{31} & \lambda_3^2 f_{32} & \dots & \lambda_3^{n-1} f_{31} & \lambda_3^n f_{32} \\ \vdots & \vdots \\ f_{2n1} & f_{2n2} & \lambda_{2n} f_{2n1} & \lambda_{2n} f_{2n2} & \lambda_{2n}^2 f_{2n1} & \lambda_{2n}^2 f_{2n2} & \dots & \lambda_{2n}^{n-1} f_{2n1} & \lambda_{2n}^n f_{2n2} \end{vmatrix}.$$

It is easy to construct a simple form of the determinant of T_n

$$\det(T_n) = (\lambda - \lambda_1)(\lambda - \lambda_2) \cdots (\lambda - \lambda_{2n-1})(\lambda - \lambda_{2n})$$

Next, we consider the transformed new solutions $(E^{[n]}, p^{[n]}, \eta^{[n]})$ of NLS-MB equations corresponding to the n-fold DT.

Corollary 1. For the n-fold DT, the transformed potentials are

$$\begin{aligned} U_0^{[n]} &= U_0 - [\sigma_3, T_n], \\ V_{-1}^{[n]} &= T_n|_{\lambda=i\omega_0} V_{-1} T_n^{-1}|_{\lambda=i\omega_0}, \end{aligned} \tag{17}$$

which leads to the new solutions $E^{[n]}, p^{[n]}$ and $\eta^{[n]}$ of the form

$$E^{[n]} = E - 2(t_1)_{12}, \tag{18}$$

$$p^{[n]} = -\frac{1}{\det(T_n)} (-2\eta(T_n)_{11}(T_n)_{12} + p^*(T_n)_{12}(T_n)_{12} - p(T_n)_{11}(T_n)_{11})|_{\lambda=i\omega_0}, \tag{19}$$

$$\eta^{[n]} = \frac{1}{\det(T_n)} (\eta((T_n)_{11}(T_n)_{22} + (T_n)_{12}(T_n)_{21}) - p^*(T_n)_{12}(T_n)_{22} + p(T_n)_{11}(T_n)_{21})|_{\lambda=i\omega_0}, \tag{20}$$

and the new eigenfunction $f_k^{[n]}$ of λ_k is

$$f_k^{[n]} = \begin{pmatrix} f_{k1} & f_{k2} & \lambda_k f_{k1} & \lambda_k f_{k2} & \lambda_k^2 f_{k1} & \lambda_k^2 f_{k2} & \dots & \lambda_k^{n-1} f_{k1} & \lambda_k^{n-1} f_{k2} & \lambda_k^n f_{k1} \\ f_{11} & f_{12} & \lambda_1 f_{11} & \lambda_1 f_{12} & \lambda_1^2 f_{11} & \lambda_1^2 f_{12} & \dots & \lambda_1^{n-1} f_{11} & \lambda_1^{n-1} f_{12} & \lambda_1^n f_{11} \\ f_{21} & f_{22} & \lambda_2 f_{21} & \lambda_2 f_{22} & \lambda_2^2 f_{21} & \lambda_2^2 f_{22} & \dots & \lambda_2^{n-1} f_{21} & \lambda_2^{n-1} f_{22} & \lambda_2^n f_{21} \\ f_{31} & f_{32} & \lambda_3 f_{31} & \lambda_3 f_{32} & \lambda_3^2 f_{31} & \lambda_3^2 f_{32} & \dots & \lambda_3^{n-1} f_{31} & \lambda_3^{n-1} f_{32} & \lambda_3^n f_{31} \\ \vdots & \vdots \\ f_{2n1} & f_{2n2} & \lambda_{2n} f_{2n1} & \lambda_{2n} f_{2n2} & \lambda_{2n}^2 f_{2n1} & \lambda_{2n}^2 f_{2n2} & \dots & \lambda_{2n}^{n-1} f_{2n1} & \lambda_{2n}^{n-1} f_{2n2} & \lambda_{2n}^n f_{2n1} \end{pmatrix} \begin{pmatrix} |W_{2n}| \\ f_{k1} & f_{k2} & \lambda_k f_{k1} & \lambda_k f_{k2} & \lambda_k^2 f_{k1} & \lambda_k^2 f_{k2} & \dots & \lambda_k^{n-1} f_{k1} & \lambda_k^{n-1} f_{k2} & \lambda_k^n f_{k2} \\ f_{11} & f_{12} & \lambda_1 f_{11} & \lambda_1 f_{12} & \lambda_1^2 f_{11} & \lambda_1^2 f_{12} & \dots & \lambda_1^{n-1} f_{11} & \lambda_1^{n-1} f_{12} & \lambda_1^n f_{12} \\ f_{21} & f_{22} & \lambda_2 f_{21} & \lambda_2 f_{22} & \lambda_2^2 f_{21} & \lambda_2^2 f_{22} & \dots & \lambda_2^{n-1} f_{21} & \lambda_2^{n-1} f_{22} & \lambda_2^n f_{22} \\ f_{31} & f_{32} & \lambda_3 f_{31} & \lambda_3 f_{32} & \lambda_3^2 f_{31} & \lambda_3^2 f_{32} & \dots & \lambda_3^{n-1} f_{31} & \lambda_3^{n-1} f_{32} & \lambda_3^n f_{32} \\ \vdots & \vdots \\ f_{2n1} & f_{2n2} & \lambda_{2n} f_{2n1} & \lambda_{2n} f_{2n2} & \lambda_{2n}^2 f_{2n1} & \lambda_{2n}^2 f_{2n2} & \dots & \lambda_{2n}^{n-1} f_{2n1} & \lambda_{2n}^{n-1} f_{2n2} & \lambda_{2n}^n f_{2n2} \end{pmatrix} \begin{pmatrix} |W_{2n}| \\ |W_{2n}| \end{pmatrix}.$$

Note that

$$\lambda_{2k} = -\lambda_{2k-1}^*, f_{2k} = \begin{pmatrix} -f_{2k-12}^* \\ f_{2k-11}^* \end{pmatrix} \quad (21)$$

in order to satisfy the constraints of DT.

3. N-ORDER BRIGHT AND DARK ROGUE WAVES GENERATED BY N-ORDER BREATHER SOLUTIONS

By using the results of DT discussed above, breather solutions of E , p and η of NLS-MB equations are generated by assuming a periodic seed solution. Then we can construct the explicit bright and dark rogue waves of the NLS-MB equations through a Taylor series expansion of the breather solutions.

Substituting, $E = d \exp[i\rho]$, $p = i f E$, $\eta = 1$ into the spectral problem eq.(3) and eq.(4), and using the method of separation of variables and the superposition principle, the eigenfunction f_{2k-1} associated with λ_{2k-1} is given by

$$\begin{pmatrix} f_{2k-11}(x, t, \lambda_{2k-1}) \\ f_{2k-12}(x, t, \lambda_{2k-1}) \end{pmatrix} = \begin{pmatrix} C_1 \varpi(x, t, \lambda_{2k-1})[1, 2k-1] - C_2 \varpi^*(x, t, -\lambda_{2k-1}^*)[2, 2k-1] \\ C_1 \varpi(x, t, \lambda_{2k-1})[2, 2k-1] + C_2 \varpi^*(x, t, -\lambda_{2k-1}^*)[1, 2k-1] \end{pmatrix}. \quad (22)$$

Here

$$\begin{aligned} \begin{pmatrix} \varpi(x, t, \lambda_{2k-1})[1, 2k-1] \\ \varpi(x, t, \lambda_{2k-1})[2, 2k-1] \end{pmatrix} &= \begin{pmatrix} d \exp[\frac{i}{2}\rho + ic(\lambda_{2k-1})] \\ [i(c_1(\lambda_{2k-1}) + \frac{b}{2}) - \lambda_{2k-1}] \exp[-\frac{i}{2}\rho + ic(\lambda_{2k-1})] \end{pmatrix}, \\ \varpi(x, t, \lambda_{2k-1}) &= \begin{pmatrix} \varpi(x, t, \lambda_{2k-1})[1, 2k-1] \\ \varpi(x, t, \lambda_{2k-1})[2, 2k-1] \end{pmatrix}. \end{aligned}$$

Note that $\varpi(x, t, \lambda_{2k-1})$ is the basic solution of the spectral problem eq.(3) and eq.(4). Here $a, b, d, t, z \in \mathbb{R}$, $C_1, C_2 \in \mathbb{C}$,

$$\begin{aligned} c(\lambda_{2k-1}) &= c_1(\lambda_{2k-1})x + c_2(\lambda_{2k-1})t, \\ c_1(\lambda_{2k-1}) &= \sqrt{d^2 - (\frac{ib}{2} - \lambda_{2k-1})^2}, \\ c_2(\lambda_{2k-1}) &= \left(i\lambda_{2k-1} - \frac{b}{2} - \frac{if}{\lambda_{2k-1} - i\omega_0} \right) c_1(\lambda_{2k-1}), \\ \rho &= a t + b x, \end{aligned}$$

$$f = \frac{1}{2}(a + \frac{b^2}{2} - d^2),$$

and the $(-b + 2\omega_0)f = 2$ is used for f .

3.1 The n-order breather solutions of NLS-MB equations

For simplicity, under the condition $C_1 = C_2 = 1$, let $\lambda_{2k-1} = \alpha_{2k-1} + i\frac{b}{2}$, such that $\text{Im}(\frac{ib}{2} - \lambda_{2k-1}) = 0$ and $c_1(\lambda_{2k-1}) = \sqrt{d^2 - \text{Re}^2(\lambda_{2k-1})} \in \mathbb{R}$, and using eq. (21), then substituting eigenfunctions eq. (22) into eq. (16), we obtain the determinant representation of DT in the form

$$T_n = T_n(\lambda; \lambda_1, \lambda_2, \dots, \lambda_{2n-1}, \lambda_{2n}) = \begin{pmatrix} \widehat{(T_n)_{11}} & \widehat{(T_n)_{12}} \\ \widehat{(T_n)_{21}} & \widehat{(T_n)_{22}} \end{pmatrix}, \quad (23)$$

with

$$\begin{aligned} \bar{W}_{2n} &= \begin{pmatrix} 1 & \gamma_1 & \lambda_1 & \lambda_1\gamma_1 & \lambda_1^2 & \dots & \lambda_1^{n-1} & \lambda_1^{n-1}\gamma_1 \\ -\gamma_1^* & 1 & \lambda_1^*\gamma_1^* & -\lambda_1^* & -\lambda_1^{*2}\gamma_1^* & \dots & -(-\lambda_1^*)^{n-1}\gamma_1^* & (-\lambda_1^*)^{n-1} \\ 1 & \gamma_3 & \lambda_3 & \lambda_3\gamma_3 & \lambda_3^2 & \dots & \lambda_3^{n-1} & \lambda_3^{n-1}\gamma_3 \\ \vdots & \vdots \\ -\gamma_{2n-1}^* & 1 & \lambda_{2n-1}^*\gamma_{2n-1}^* & -\lambda_{2n-1}^* & -\lambda_{2n-1}^{*2}\gamma_{2n-1}^* & \dots & -(-\lambda_{2n-1}^*)^{n-1}\gamma_{2n-1}^* & (-\lambda_{2n-1}^*)^{n-1} \end{pmatrix}, \\ \widehat{(T_n)_{11}} &= \begin{vmatrix} 1 & 0 & \lambda & \dots & \lambda^{n-1} & 0 & \lambda^n \\ 1 & \gamma_1 & \lambda_1 & \dots & \lambda_1^{n-1} & \lambda_1^{n-1}\gamma_1 & \lambda_1^n \\ -\gamma_1^* & 1 & \lambda_1^*\gamma_1^* & \dots & -(-\lambda_1^*)^{n-1}\gamma_1^* & (-\lambda_1^*)^{n-1} & -(-\lambda_1^*)^n\gamma_1^* \\ 1 & \gamma_3 & \lambda_3 & \dots & \lambda_3^{n-1} & \lambda_3^{n-1}\gamma_3 & \lambda_3^n \\ \vdots & \vdots & \vdots & \vdots & \vdots & \vdots & \vdots \\ -\gamma_{2n-1}^* & 1 & \lambda_{2n-1}^*\gamma_{2n-1}^* & \dots & -(-\lambda_{2n-1}^*)^{n-1}\gamma_{2n-1}^* & (-\lambda_{2n-1}^*)^{n-1} & -(-\lambda_{2n-1}^*)^n\gamma_{2n-1}^* \end{vmatrix}, \\ \widehat{(T_n)_{12}} &= \begin{vmatrix} 0 & 1 & 0 & \dots & 0 & \lambda^{n-1} & 0 \\ 1 & \gamma_1 & \lambda_1 & \dots & \lambda_1^{n-1} & \lambda_1^{n-1}\gamma_1 & \lambda_1^n \\ -\gamma_1^* & 1 & \lambda_1^*\gamma_1^* & \dots & -(-\lambda_1^*)^{n-1}\gamma_1^* & (-\lambda_1^*)^{n-1} & -(-\lambda_1^*)^n\gamma_1^* \\ 1 & \gamma_3 & \lambda_3 & \dots & \lambda_3^{n-1} & \lambda_3^{n-1}\gamma_3 & \lambda_3^n \\ \vdots & \vdots & \vdots & \vdots & \vdots & \vdots & \vdots \\ -\gamma_{2n-1}^* & 1 & \lambda_{2n-1}^*\gamma_{2n-1}^* & \dots & -(-\lambda_{2n-1}^*)^{n-1}\gamma_{2n-1}^* & (-\lambda_{2n-1}^*)^{n-1} & -(-\lambda_{2n-1}^*)^n\gamma_{2n-1}^* \end{vmatrix}, \\ \widehat{(T_n)_{21}} &= \begin{vmatrix} 1 & 0 & \lambda & \dots & \lambda^{n-1} & 0 & 0 \\ 1 & \gamma_1 & \lambda_1 & \dots & \lambda_1^{n-1} & \lambda_1^{n-1}\gamma_1 & \lambda_1^n\gamma_1 \\ -\gamma_1^* & 1 & \lambda_1^*\gamma_1^* & \dots & -(-\lambda_1^*)^{n-1}\gamma_1^* & (-\lambda_1^*)^{n-1} & (-\lambda_1^*)^n \\ 1 & \gamma_3 & \lambda_3 & \dots & \lambda_3^{n-1} & \lambda_3^{n-1}\gamma_3 & \lambda_3^n\gamma_3 \\ \vdots & \vdots & \vdots & \vdots & \vdots & \vdots & \vdots \\ -\gamma_{2n-1}^* & 1 & \lambda_{2n-1}^*\gamma_{2n-1}^* & \dots & -(-\lambda_{2n-1}^*)^{n-1}\gamma_{2n-1}^* & (-\lambda_{2n-1}^*)^{n-1} & -(-\lambda_{2n-1}^*)^n\gamma_{2n-1}^* \end{vmatrix}, \end{aligned}$$

$$\widehat{(T_n)_{22}} = \begin{vmatrix} 0 & 1 & 0 & \dots & 0 & \lambda^{n-1} & \lambda^n \\ 1 & \gamma_1 & \lambda_1 & \dots & \lambda_1^{n-1} & \lambda_1^{n-1}\gamma_1 & \lambda_1^n\gamma_1 \\ -\gamma_1^* & 1 & \lambda_1^*\gamma_1^* & \dots & -(-\lambda_1^*)^{n-1}\gamma_1^* & (-\lambda_1^*)^{n-1} & (-\lambda_1^*)^n \\ 1 & \gamma_3 & \lambda_3 & \dots & \lambda_3^{n-1} & \lambda_3^{n-1}\gamma_3 & \lambda_3^n\gamma_3 \\ \vdots & \vdots & \vdots & \vdots & \vdots & \vdots & \vdots \\ -\gamma_{2n-1}^* & 1 & \lambda_{2n-1}^*\gamma_{2n-1}^* & \dots & -(-\lambda_{2n-1}^*)^{n-1}\gamma_{2n-1}^* & (-\lambda_{2n-1}^*)^{n-1} & (-\lambda_{2n-1}^*)^n \end{vmatrix},$$

$$\widehat{(Q_n)_{11}} = \begin{vmatrix} 1 & \gamma_1 & \lambda_1 & \lambda_1\gamma_1 & \lambda_1^2 & \dots & \lambda_1^{n-1}\gamma_1 & \lambda_1^n \\ -\gamma_1^* & 1 & \lambda_1^*\gamma_1^* & -\lambda_1^* & -\lambda_1^{*2}\gamma_1^* & \dots & (-\lambda_1^*)^{n-1} & -(-\lambda_1^*)^n\gamma_1^* \\ 1 & \gamma_3 & \lambda_3 & \lambda_3\gamma_3 & \lambda_3^2 & \dots & \lambda_3^{n-1}\gamma_3 & \lambda_3^n \\ \vdots & \vdots \\ -\gamma_{2n-1}^* & 1 & \lambda_{2n-1}^*\gamma_{2n-1}^* & -\lambda_{2n-1}^* & -\lambda_{2n-1}^{*2}\gamma_{2n-1}^* & \dots & (-\lambda_{2n-1}^*)^{n-1} & -(-\lambda_{2n-1}^*)^n\gamma_{2n-1}^* \end{vmatrix},$$

$$\widehat{(Q_n)_{12}} = \begin{vmatrix} 1 & \gamma_1 & \lambda_1 & \lambda_1\gamma_1 & \dots & \lambda_1^{n-1} & \lambda_1^n \\ -\gamma_1^* & 1 & \lambda_1^*\gamma_1^* & -\lambda_1^* & \dots & -(-\lambda_1^*)^{n-1}\gamma_1^* & -(-\lambda_1^*)^n\gamma_1^* \\ 1 & \gamma_3 & \lambda_3 & \lambda_3\gamma_3 & \dots & \lambda_3^{n-1} & \lambda_3^n \\ \vdots & \vdots & \vdots & \vdots & \vdots & \vdots & \vdots \\ -\gamma_{2n-1}^* & 1 & \lambda_{2n-1}^*\gamma_{2n-1}^* & -\lambda_{2n-1}^* & \dots & -(-\lambda_{2n-1}^*)^{n-1}\gamma_{2n-1}^* & -(-\lambda_{2n-1}^*)^n\gamma_{2n-1}^* \end{vmatrix},$$

$$\widehat{(Q_n)_{21}} = \begin{vmatrix} 1 & \gamma_1 & \lambda_1 & \lambda_1\gamma_1 & \lambda_1^2 & \dots & \lambda_1^{n-1}\gamma_1 & \lambda_1^n\gamma_1 \\ -\gamma_1^* & 1 & \lambda_1^*\gamma_1^* & -\lambda_1^* & -\lambda_1^{*2}\gamma_1^* & \dots & (-\lambda_1^*)^{n-1} & (-\lambda_1^*)^n \\ 1 & \gamma_3 & \lambda_3 & \lambda_3\gamma_3 & \lambda_3^2 & \dots & \lambda_3^{n-1}\gamma_3 & \lambda_3^n\gamma_3 \\ \vdots & \vdots \\ -\gamma_{2n-1}^* & 1 & \lambda_{2n-1}^*\gamma_{2n-1}^* & -\lambda_{2n-1}^* & -\lambda_{2n-1}^{*2}\gamma_{2n-1}^* & \dots & (-\lambda_{2n-1}^*)^{n-1} & (-\lambda_{2n-1}^*)^n \end{vmatrix},$$

$$\widehat{(Q_n)_{22}} = \begin{vmatrix} 1 & \gamma_1 & \lambda_1 & \lambda_1\gamma_1 & \lambda_1^2 & \dots & \lambda_1^{n-1} & \lambda_1^n\gamma_1 \\ -\gamma_1^* & 1 & \lambda_1^*\gamma_1^* & -\lambda_1^* & -\lambda_1^{*2}\gamma_1^* & \dots & -(-\lambda_1^*)^{n-1}\gamma_1^* & (-\lambda_1^*)^n \\ 1 & \gamma_3 & \lambda_3 & \lambda_3\gamma_3 & \lambda_3^2 & \dots & \lambda_3^{n-1} & \lambda_3^n\gamma_3 \\ \vdots & \vdots \\ -\gamma_{2n-1}^* & 1 & \lambda_{2n-1}^*\gamma_{2n-1}^* & -\lambda_{2n-1}^* & -\lambda_{2n-1}^{*2}\gamma_{2n-1}^* & \dots & -(-\lambda_{2n-1}^*)^{n-1}\gamma_{2n-1}^* & (-\lambda_{2n-1}^*)^n \end{vmatrix}.$$

Here

$$\gamma_{2k-1} = \frac{v_1}{v_2}, \quad (24)$$

$$\begin{aligned} v_1 &= (2i(\alpha_{2k-1}^2 - d^2) \sin(\frac{\sqrt{d^2 - \alpha_{2k-1}^2}(-s_2x + s_4t)}{s_2}) \cos(\frac{\sqrt{d^2 - \alpha_{2k-1}^2}(-s_2x + s_4t)}{s_2}) \\ &+ i(-\alpha_{2k-1}^2 + d^2) \sin(\frac{2\sqrt{d^2 - \alpha_{2k-1}^2}(-s_2x + s_4t)}{s_2}) - 2d\alpha_{2k-1} \cosh(\frac{2\sqrt{d^2 - \alpha_{2k-1}^2}s_3t}{s_2}) \\ &+ 2d^2 \cos(\frac{2\sqrt{d^2 - \alpha_{2k-1}^2}(-s_2x + s_4t)}{s_2}) + 2id \sinh(\frac{2\sqrt{d^2 - \alpha_{2k-1}^2}s_3t}{s_2}) \sqrt{d^2 - \alpha_{2k-1}^2}) \exp(-is_1), \\ v_2 &= ((-2d^2 + 2\alpha_{2k-1}^2) \sinh(\frac{\sqrt{d^2 - \alpha_{2k-1}^2}s_3t}{s_2}) \cosh(\frac{\sqrt{d^2 - \alpha_{2k-1}^2}s_3t}{s_2}) + 2d^2 \cosh(\frac{2\sqrt{d^2 - \alpha_{2k-1}^2}s_3t}{s_2}) \\ &+ (d^2 - \alpha_{2k-1}^2) \sinh(\frac{2\sqrt{d^2 - \alpha_{2k-1}^2}s_3t}{s_2}) - 2\sqrt{d^2 - \alpha_{2k-1}^2}d \sin(\frac{2\sqrt{d^2 - \alpha_{2k-1}^2}(-s_2x + s_4t)}{s_2}) \\ &- 2d\alpha_{2k-1} \cos(\frac{2\sqrt{d^2 - \alpha_{2k-1}^2}(-s_2x + s_4t)}{s_2}), \end{aligned}$$

$$\begin{aligned}
s_1 &= \frac{-b(1/2b - \omega_0)x + (2 + 2(1/2b - \omega_0)(1/4b^2 - 1/2d^2))t}{-1/2b + \omega_0}, \\
s_2 &= (-1/2b + \omega_0)((1/2b - \omega_0)^2 + d^2), \\
s_3 &= -d\omega_0(d^2 + \omega_0^2) - 3/2db\omega_0(1/2b - \omega_0) + 1/2db(d^2 + 1/4b^2) + d, \\
s_4 &= -1/2b^2(d^2 + 1/4b^2) + b\omega_0(d^2 + \omega_0^2) + 3/2b^2\omega_0(1/2b - \omega_0) + 1/2b - \omega_0.
\end{aligned}$$

Using eq. (23) into eq.(18,19,20) with the choice in eq.(24), we can construct $E^{[n]}, p^{[n]}$ and $\eta^{[n]}$. For brevity, in the following, we are giving only an explicit expression of $E^{[1]}$ with specific parameters $d = 1, b = 2, \omega_0 = \frac{1}{2}$.

$$\begin{aligned}
E^{[1]} &= E + 4\alpha_1 \frac{v_3}{v_4} \exp(i(-5t + 2x)), \\
v_3 &= -\alpha_1 \cos(2w_1) + (2\cos(w_1) + 2\sqrt{1 - \alpha_1^2} \sin(w_1)\alpha_1 + 2\alpha_1^2 \cos(w_1)) \cosh(w_2) \\
&\quad + (2i\alpha_1^2 \sin(w_1) - 2i\sin(w_1) - 2i\alpha_1 \cos(w_1)\sqrt{1 - \alpha_1^2}) \sinh(w_2) - 2\alpha_1 - \sqrt{1 - \alpha_1^2} \sin(2w_1) \\
&\quad + i\sqrt{1 - \alpha_1^2} \sinh(2w_2) - \alpha_1 \cosh(2w_2), \\
v_4 &= 2\alpha_1^2 \cos(2w_1) - 2(4\alpha_1 \cos(w_1) + 2\sin(w_1)\sqrt{1 - \alpha_1^2}) \cosh(w_2) \\
&\quad - 2(-1 - \alpha_1^2 - \cosh(2w_2) - \sqrt{1 - \alpha_1^2}\alpha_1 \sin(2w_1)), \\
w_1 &= -2\sqrt{1 - \alpha_1^2}x + \frac{12}{5}\sqrt{1 - \alpha_1^2}t, w_2 = \frac{26}{5}\sqrt{1 - \alpha_1^2}t. \tag{25}
\end{aligned}$$

The dynamical evolution of $|E^{[1]}|^2$, $|p^{[1]}|^2$ and $\eta^{[1]}$ for the parametric choice $d = 1, b = 2, \omega_0 = \frac{1}{2}, \alpha_1 = 0.8$ are plotted in the Figures 1-3, which confirms the direct verification of the periodic as well as decaying properties of typical breather solutions. The breather of $E^{[1]}$ is almost same as that of the NLS equation, which has one upper peak and two caves in each periodic unit. On the other hand, we observe that there are two new kinds of breathers for $p^{[1]}$ and $\eta^{[1]}$. It is interesting to note that new breather $p^{[1]}$ admit one upper ring and three down peaks in each periodic unit. Whereas the new breather $\eta^{[1]}$ has two lumps and one down peak in each periodic unit. Moreover, these two new breathers can be called as dark breathers because the down amplitude is dominant in both the cases. The above discussed new properties are clearly seen in Figures 1-3.

3.2 The first-order rogue waves generated by first-order breather solutions above

Similarly, under the condition $C_1 = C_2 = 1$, substituting eigenfunctions eq.(22) into eqs.(18,19,20) with $\lambda_1 = \alpha_1 + i\frac{b}{2}$, by assuming $\alpha_1 \rightarrow d(d > 0)$, $E^{[1]}, p^{[1]}$ and $\eta^{[1]}$ become rational solutions $\{\tilde{E}^{[1]}, \tilde{p}^{[1]}, \tilde{\eta}^{[1]}\}$ in the form of rogue waves [53]. When $x \rightarrow \infty, t \rightarrow \infty$ in the above expressions, after some manipulations, we find $|\tilde{E}^{[1]}|^2 \rightarrow d^2$, $|\tilde{p}^{[1]}|^2 \rightarrow \frac{d^2}{(\frac{b}{2} - \omega_0)^2}$ and $\tilde{\eta}^{[1]} \rightarrow 1$. In addition to the above conditions, from $|\tilde{E}^{[1]}|_x^2 = 0$ and $|\tilde{E}^{[1]}|_t^2 = 0$, we also observe that the maximum amplitude of $|\tilde{E}^{[1]}|^2$ occurs at $t = 0$ and $x = 0$ and is equal to $9d^2$, and the minimum amplitude of $|\tilde{E}^{[1]}|^2$ occurs at $t = 0$ and $x = \pm\frac{\sqrt{3}}{2d}$ and is equal to 0. By using similar procedure discussed above, we can also obtain the extreme value of $|\tilde{p}^{[1]}|^2$ and $\tilde{\eta}^{[1]}$.

Figure 4 is plotted for the rogue wave $|\tilde{E}^{[1]}|^2$ with specific parameters $d = 1, b = 2, \omega_0 = \frac{1}{2}$. From figure 4, we infer the following interesting results: 1) the $|\tilde{E}^{[1]}|^2 \rightarrow 1$ by assuming $x \rightarrow \infty, t \rightarrow \infty$ which gives the asymptotic plane; 2) The maximum amplitude of $|\tilde{E}^{[1]}|^2$ occurs at $t = 0$ and $x = 0$

and is equal to 9, and the minimum amplitude of $|\tilde{E}^{[1]}|^2$ occurs at $t = 0$ and $x = \pm \frac{\sqrt{3}}{2}$ and is equal to 0. As the general expression of the extreme values of $|p^{[1]}|^2$ and $\tilde{\eta}^{[1]}$ are quite complicated in nature, for simplicity, we only discuss these solutions under certain choice of parameters.

Figure 5 is plotted for the rogue wave $|\tilde{p}^{[1]}|^2$ on $(x - t)$ plane with the above parameters. Like in the earlier case, here also we observe the following salient features: 1) the height of the asymptotical plane is 4 because $|\tilde{p}^{[1]}|^2 \rightarrow 4$, when $x \rightarrow \infty, t \rightarrow \infty$; 2) The maximum amplitude of $|\tilde{p}^{[1]}|^2$ occurs in the form of ring curve on $(x - t)$ plane defined by $-\frac{507}{16}t^2 + \frac{1681}{8}t^4 + \frac{25}{8}x^4 - \frac{55}{128} + \frac{65}{16}x^2 + \frac{277}{4}x^2t^2 - 15x^3t + \frac{65}{4}xt - 123xt^3 = 0$, and is equal to 5, and the minimum amplitude of $|\tilde{p}^{[1]}|^2$ occurs at four points $\{(t = \frac{+5 + \sqrt{5}}{52}, x = \frac{+19 + 9\sqrt{5}}{52}), (t = \frac{+5 - \sqrt{5}}{52}, x = \frac{+19 - 9\sqrt{5}}{52}), (t = \frac{-5 + \sqrt{5}}{52}, x = \frac{-19 + 9\sqrt{5}}{52}), (t = \frac{-5 - \sqrt{5}}{52}, x = \frac{-19 - 9\sqrt{5}}{52})\}$ and is equal to 0; 3) the extreme value of the amplitude $|\tilde{p}^{[1]}|^2$ occurs at $t = 0$ and $x = 0$ and is equal to $\frac{4}{25}$. We also observe that the middle down peak in Figure 5 has two sub-peaks. Due to the direction of the observation of the figure, these two close sub-peaks are not clearly distinguished from the figure, we just find three down peaks.

Figure 6 is plotted for the rogue wave $\tilde{\eta}^{[1]}$ with specific parameters as in fig.4. From the Figure, we observe the following new results: 1) the height of the asymptotical plane is 1 because $\tilde{\eta}^{[1]} \rightarrow 1$ by letting $x \rightarrow \infty, t \rightarrow \infty$; 2) the maximum amplitude of $\tilde{\eta}^{[1]}$ occurs at two points $\{(t = \frac{+5 + \sqrt{5}}{52}, x = \frac{+19 + 9\sqrt{5}}{52})\}$ and $\{(t = \frac{-5 + \sqrt{5}}{52}, x = \frac{-19 + 9\sqrt{5}}{52})\}$ and is equal to $\sqrt{5}$, and the minimum amplitude of $\tilde{\eta}^{[1]}$ occurs at two points $\{(t = \frac{+5 - \sqrt{5}}{52}, x = \frac{+19 - 9\sqrt{5}}{52})\}$ and $\{(t = \frac{-5 + \sqrt{5}}{52}, x = \frac{-19 + 9\sqrt{5}}{52})\}$ and is equal to $-\sqrt{5}$; 3) the extreme value of the amplitude $\tilde{\eta}^{[1]}$ occurs at $t = 0$ and $x = 0$ and is equal to $-\frac{11}{5}$. Like in Figure.5, here also we observe that the down peak in Figure 6 has two sub-peaks.

3.3 The higher order rogue waves and their determinant forms

In order to emphasize the richness of the higher order rogue waves, we can modify C_1 and C_2 in the equation (22) as the following:

$$\begin{aligned} C_1 &= K_0 + \exp(ic_1(\lambda_{2k-1}) \sum_{j=0}^{k-1} J_j (\lambda_{2k-1} - (d + i\frac{b}{2}))^j) \\ C_2 &= K_0 + \exp(-ic_1(\lambda_{2k-1}) \sum_{j=0}^{k-1} J_j (\lambda_{2k-1} - (d + i\frac{b}{2}))^j) \end{aligned} \quad (26)$$

Here $K_0, J_j \in \mathbb{C}$. Note that $\lambda_{2k-1} = d + i\frac{b}{2}$ is the zero point of $c_1(\lambda_{2k-1})$.

Based on the section 3.2, higher order rogue waves can be constructed by the breather solutions. In other words, let $\lambda_{2k-1} \rightarrow d + i\frac{b}{2}$ in n-order breather solutions, n-order rogue waves can be given. Generally, in comparison to the method of limiting the breather solutions, the method of making rational eigenfunction below may be more direct and the rogue wave can be shown by determinant forms.

Substituting eq.(26) into eqs.(22), by assuming $\lambda_{2k-1} \rightarrow d + i\frac{b}{2}$, eigenfunction f_{2k-1} associated with λ_{2k-1} become rational eigenfunction f_r as follows.

$$\begin{pmatrix} f_{r1} \\ f_{r2} \end{pmatrix} = \begin{pmatrix} -((2dK_0 + 2d)x + 2(\frac{2i}{(b - 2\omega_0)(d + \frac{1}{2}ib - i\omega_0)} + id - b)(K_0 + 1)dt + 2J_0d + K_0 + 1)\sqrt{2d}\exp(K) \\ -(-(2dK_0 + 2d)x - 2(\frac{2i}{(b - 2\omega_0)(d + \frac{1}{2}ib - i\omega_0)} + id - b)(K_0 + 1)dt - 2J_0d + K_0 + 1)\sqrt{2d}\exp(-K) \end{pmatrix},$$

$$K = \frac{1}{2}i(-\frac{8 + b^3 - 2b^2\omega_0 - 2d^2b + 4d^2\omega_0}{2(b - 2\omega_0)}t + bx) \quad (27)$$

Substituting eigenfunctions eq.(27) into eqs.(11,12,13), we can get the first order rogue waves $\{\bar{E}^{[1]}, \bar{p}^{[1]}, \bar{\eta}^{[1]}\}$ in the form of determinant. The dynamical evolution of $|\bar{E}^{[1]}|^2$, $|\bar{p}^{[1]}|^2$ and $\bar{\eta}^{[1]}$ for the parametric choice d, b, ω_0, K_0, J_0 are respectively similar to the Figures 4-6, but we can control the position of the first-order rogue waves by choosing the parameters K_0 and J_0 .

Theorem 2. For the n-fold DT, the n-order rogue waves $\bar{E}^{[n]}, \bar{p}^{[n]}$ and $\bar{\eta}^{[n]}$ of the form

$$\bar{E}^{[n]} = E - 2(\bar{t}_{r1})_{12}, \quad (28)$$

$$\bar{p}^{[n]} = -\frac{1}{\det(\bar{T}_{rn})}(-2\eta(\bar{T}_{rn})_{11}(\bar{T}_{rn})_{12} + p^*(\bar{T}_{rn})_{12}(\bar{T}_{rn})_{12} - p(\bar{T}_{rn})_{11}(\bar{T}_{rn})_{11})|_{\lambda=i\omega_0}, \quad (29)$$

$$\bar{\eta}^{[n]} = \frac{1}{\det(\bar{T}_{rn})}(\eta((\bar{T}_{rn})_{11}(\bar{T}_{rn})_{22} + (\bar{T}_{rn})_{12}(\bar{T}_{rn})_{21}) - p^*(\bar{T}_{rn})_{12}(\bar{T}_{rn})_{22} + p(\bar{T}_{rn})_{11}(\bar{T}_{rn})_{21})|_{\lambda=i\omega_0}, \quad (30)$$

The final form of $\bar{T}_{rn}(\lambda)$ has the form,

$$\bar{T}_{rn} = \bar{T}_{rn}(\lambda) = \begin{pmatrix} \widetilde{(\bar{T}_{rn})_{11}} & \widetilde{(\bar{T}_{rn})_{12}} \\ \frac{\widetilde{(\bar{T}_{rn})_{11}}}{|W_{r2n}|} & \frac{\widetilde{(\bar{T}_{rn})_{12}}}{|W_{r2n}|} \\ \frac{\widetilde{(\bar{T}_{rn})_{21}}}{|W_{r2n}|} & \frac{\widetilde{(\bar{T}_{rn})_{22}}}{|W_{r2n}|} \end{pmatrix}, \quad (31)$$

$$\bar{t}_{r1} = \begin{pmatrix} \frac{\widetilde{(\bar{T}_{rn})_{11}}}{|W_{r2n}|} & \frac{\widetilde{(\bar{T}_{rn})_{12}}}{|W_{r2n}|} \\ \frac{\widetilde{(\bar{T}_{rn})_{21}}}{|W_{r2n}|} & \frac{\widetilde{(\bar{T}_{rn})_{22}}}{|W_{r2n}|} \end{pmatrix},$$

$$W_{r2n} = \begin{pmatrix} h_{01}^1 & h_{02}^1 & h_{11}^1 & h_{12}^1 & \dots & h_{n-11}^1 & h_{n-12}^1 \\ -h_{02}^1 & h_{01}^1 & h_{12}^1 & -h_{11}^1 & \dots & (-1)^n h_{n-12}^1 & (-1)^{n-1} h_{n-11}^1 \\ h_{01}^3 & h_{02}^3 & h_{11}^3 & h_{12}^3 & \dots & h_{n-11}^3 & h_{n-12}^3 \\ \vdots & \vdots & \vdots & \vdots & \vdots & \vdots & \vdots \\ -h_{02}^{2n-1} & h_{01}^{2n-1} & h_{12}^{2n-1} & -h_{11}^{2n-1} & \dots & (-1)^n h_{n-12}^{2n-1} & (-1)^{n-1} h_{n-11}^{2n-1} \end{pmatrix},$$

$$\widetilde{(\bar{T}_{rn})_{11}} = \begin{vmatrix} 1 & 0 & \lambda & 0 & \dots & \lambda^{n-1} & 0 & \lambda^n \\ h_{01}^1 & h_{02}^1 & h_{11}^1 & h_{12}^1 & \dots & h_{n-11}^1 & h_{n-12}^1 & h_{n1}^1 \\ -h_{02}^1 & h_{01}^1 & h_{12}^1 & -h_{11}^1 & \dots & (-1)^n h_{n-12}^1 & (-1)^{n-1} h_{n-11}^1 & (-1)^{n+1} h_{n2}^1 \\ h_{01}^3 & h_{02}^3 & h_{11}^3 & h_{12}^3 & \dots & h_{n-11}^3 & h_{n-12}^3 & h_{n1}^3 \\ \vdots & \vdots \\ -h_{02}^{2n-1} & h_{01}^{2n-1} & h_{12}^{2n-1} & -h_{11}^{2n-1} & \dots & (-1)^n h_{n-12}^{2n-1} & (-1)^{n-1} h_{n-11}^{2n-1} & (-1)^{n+1} h_{n2}^{2n-1} \end{vmatrix},$$

$$\begin{aligned}
\widetilde{(T_{rn})}_{12} &= \begin{vmatrix} 0 & 1 & 0 & \lambda & \dots & 0 & \lambda^{n-1} & 0 \\ h_{01}^1 & h_{02}^1 & h_{11}^1 & h_{12}^1 & \dots & h_{n-11}^1 & h_{n-12}^1 & h_{n1}^1 \\ -h_{02}^{1*} & h_{01}^{1*} & h_{12}^{1*} & -h_{11}^{1*} & \dots & (-1)^n h_{n-12}^1 & (-1)^{n-1} h_{n-11}^1 & (-1)^{n+1} h_{n2}^{1*} \\ h_{01}^3 & h_{02}^3 & h_{11}^3 & h_{12}^3 & \dots & h_{n-11}^3 & h_{n-12}^3 & h_{n1}^3 \\ \vdots & \vdots \\ -h_{02}^{2n-1*} & h_{01}^{2n-1*} & h_{12}^{2n-1*} & -h_{11}^{2n-1*} & \dots & (-1)^n h_{n-12}^{2n-1*} & (-1)^{n-1} h_{n-11}^{2n-1*} & (-1)^{n+1} h_{n2}^{2n-1*} \end{vmatrix}, \\
\widetilde{(T_{rn})}_{21} &= \begin{vmatrix} 1 & 0 & \lambda & 0 & \dots & \lambda^{n-1} & 0 & 0 \\ h_{01}^1 & h_{02}^1 & h_{11}^1 & h_{12}^1 & \dots & h_{n-11}^1 & h_{n-12}^1 & h_{n2}^1 \\ -h_{02}^{1*} & h_{01}^{1*} & h_{12}^{1*} & -h_{11}^{1*} & \dots & (-1)^n h_{n-12}^1 & (-1)^{n-1} h_{n-11}^1 & (-1)^n h_{n1}^1 \\ h_{01}^3 & h_{02}^3 & h_{11}^3 & h_{12}^3 & \dots & h_{n-11}^3 & h_{n-12}^3 & h_{n2}^3 \\ \vdots & \vdots \\ -h_{02}^{2n-1*} & h_{01}^{2n-1*} & h_{12}^{2n-1*} & -h_{11}^{2n-1*} & \dots & (-1)^n h_{n-12}^{2n-1*} & (-1)^{n-1} h_{n-11}^{2n-1*} & (-1)^n h_{n1}^{2n-1*} \end{vmatrix}, \\
\widetilde{(T_{rn})}_{22} &= \begin{vmatrix} 0 & 1 & 0 & \lambda & \dots & 0 & \lambda^{n-1} & \lambda^n \\ h_{01}^1 & h_{02}^1 & h_{11}^1 & h_{12}^1 & \dots & h_{n-11}^1 & h_{n-12}^1 & h_{n2}^1 \\ -h_{02}^{1*} & h_{01}^{1*} & h_{12}^{1*} & -h_{11}^{1*} & \dots & (-1)^n h_{n-12}^1 & (-1)^{n-1} h_{n-11}^1 & (-1)^n h_{n1}^1 \\ h_{01}^3 & h_{02}^3 & h_{11}^3 & h_{12}^3 & \dots & h_{n-11}^3 & h_{n-12}^3 & h_{n2}^3 \\ \vdots & \vdots \\ -h_{02}^{2n-1*} & h_{01}^{2n-1*} & h_{12}^{2n-1*} & -h_{11}^{2n-1*} & \dots & (-1)^n h_{n-12}^{2n-1*} & (-1)^{n-1} h_{n-11}^{2n-1*} & (-1)^n h_{n1}^{2n-1*} \end{vmatrix}, \\
\widetilde{(Q_{rn})}_{11} &= \begin{vmatrix} h_{01}^1 & h_{02}^1 & h_{11}^1 & h_{12}^1 & \dots & h_{n-12}^1 & h_{n1}^1 \\ -h_{02}^{1*} & h_{01}^{1*} & h_{12}^{1*} & -h_{11}^{1*} & \dots & (-1)^{n-1} h_{n-11}^1 & (-1)^{n+1} h_{n2}^{1*} \\ h_{01}^3 & h_{02}^3 & h_{11}^3 & h_{12}^3 & \dots & h_{n-12}^3 & h_{n1}^3 \\ \vdots & \vdots & \vdots & \vdots & \vdots & \vdots & \vdots \\ -h_{02}^{2n-1*} & h_{01}^{2n-1*} & h_{12}^{2n-1*} & -h_{11}^{2n-1*} & \dots & (-1)^{n-1} h_{n-11}^{2n-1*} & (-1)^{n+1} h_{n2}^{2n-1*} \end{vmatrix}, \\
\widetilde{(Q_{rn})}_{12} &= - \begin{vmatrix} h_{01}^1 & h_{02}^1 & h_{11}^1 & h_{12}^1 & \dots & h_{n-11}^1 & h_{n1}^1 \\ -h_{02}^{1*} & h_{01}^{1*} & h_{12}^{1*} & -h_{11}^{1*} & \dots & (-1)^n h_{n-12}^1 & (-1)^{n+1} h_{n2}^{1*} \\ h_{01}^3 & h_{02}^3 & h_{11}^3 & h_{12}^3 & \dots & h_{n-11}^3 & h_{n1}^3 \\ \vdots & \vdots & \vdots & \vdots & \vdots & \vdots & \vdots \\ -h_{02}^{2n-1*} & h_{01}^{2n-1*} & h_{12}^{2n-1*} & -h_{11}^{2n-1*} & \dots & (-1)^n h_{n-12}^{2n-1*} & (-1)^{n+1} h_{n2}^{2n-1*} \end{vmatrix}, \\
\widetilde{(Q_{rn})}_{21} &= \begin{vmatrix} h_{01}^1 & h_{02}^1 & h_{11}^1 & h_{12}^1 & \dots & h_{n-12}^1 & h_{n2}^1 \\ -h_{02}^{1*} & h_{01}^{1*} & h_{12}^{1*} & -h_{11}^{1*} & \dots & (-1)^{n-1} h_{n-11}^1 & (-1)^n h_{n1}^1 \\ h_{01}^3 & h_{02}^3 & h_{11}^3 & h_{12}^3 & \dots & h_{n-12}^3 & h_{n2}^3 \\ \vdots & \vdots & \vdots & \vdots & \vdots & \vdots & \vdots \\ -h_{02}^{2n-1*} & h_{01}^{2n-1*} & h_{12}^{2n-1*} & -h_{11}^{2n-1*} & \dots & (-1)^{n-1} h_{n-11}^{2n-1*} & (-1)^n h_{n1}^{2n-1*} \end{vmatrix}, \\
\widetilde{(Q_{rn})}_{22} &= - \begin{vmatrix} h_{01}^1 & h_{02}^1 & h_{11}^1 & h_{12}^1 & \dots & h_{n-11}^1 & h_{n2}^1 \\ -h_{02}^{1*} & h_{01}^{1*} & h_{12}^{1*} & -h_{11}^{1*} & \dots & (-1)^n h_{n-12}^1 & (-1)^{n-1} h_{n1}^1 \\ h_{01}^3 & h_{02}^3 & h_{11}^3 & h_{12}^3 & \dots & h_{n-11}^3 & h_{n2}^3 \\ \vdots & \vdots & \vdots & \vdots & \vdots & \vdots & \vdots \\ -h_{02}^{2n-1*} & h_{01}^{2n-1*} & h_{12}^{2n-1*} & -h_{11}^{2n-1*} & \dots & (-1)^n h_{n-12}^{2n-1*} & (-1)^{n-1} h_{n1}^{2n-1*} \end{vmatrix}.
\end{aligned}$$

Here

$$h_{mj}^l = \frac{\partial^l}{\partial \delta^l} ((d + i\frac{b}{2} + \delta^2)^m f_{1j}(\lambda_1 = d + i\frac{b}{2} + \delta^2))|_{\delta=0}, m = 0, 1, 2, \dots, n, j = 1, 2, l = 1, 2, \dots, 2n.$$

Case 1). When $n = 2$, substituting eq.(31) into eq.(28), eq.(29) and eq.(30) can give the second-order rogue waves with five free parameters. Note that under the condition $J_1 \gg J_0$, the second-rogue can split into three first-order rogue wave (triplets rogue wave) [55] rather than two. The dynamical

evolution of $|\bar{E}^{[2]}|^2$, $|\bar{p}^{[2]}|^2$ and $\bar{\eta}^{[2]}$ for the parametric choice $d = 1, b = 2, \omega_0 = \frac{1}{2}, K_0 = 1, J_0 = 0, J_1 = 100$ are plotted in the Figures 7, 9 and 11 and their corresponding density plots are shown in the Figures 8, 10 and 12. There is another kind of second-order rogue wave, for example, $|\bar{E}^{[2]}|^2$ is higher than second-rogue above. The dynamical evolution of $|\bar{E}^{[2]}|^2$, $|\bar{p}^{[2]}|^2$ and $\bar{\eta}^{[2]}$ for the parametric choice $d = 2, b = 0, \omega_0 = \frac{1}{2}, K_0 = 1, J_0 = 0, J_1 = 0$ are plotted in the Figures 13-15. Note that eigenvalue $\lambda_1 = \lambda_3$ is real. The eigenvalue of rogue waves are different from the eigenvalue of solutions given in the past.

Case 2). When $n = 3$, substituting eq.(31) into eq.(28), eq.(29) and eq.(30) can give the third-order rogue waves with six free parameters. Note that under the condition $J_2 \gg J_i (i = 0, 1)$ or $J_1 \gg J_i (i = 0, 2)$, the third-rogue can split into six first-order rogue wave rather. Circular rogue wave [56] may be constructed by the condition $J_2 \gg J_1$ and $J_2 \gg J_0$. The dynamical evolution of $|\bar{E}^{[3]}|^2$, $|\bar{p}^{[3]}|^2$ and $\bar{\eta}^{[3]}$ for the parametric choice $d = 1, b = 2, \omega_0 = \frac{1}{2}, K_0 = 1, J_0 = 0, J_1 = 0, J_2 = 8000$ are plotted in the Figures 16-18. At the same time, triplets rogue wave may be constructed by the condition $J_1 \gg J_2$ and $J_1 \gg J_0$. The dynamical evolution of $|\bar{E}^{[3]}|^2$, $|\bar{p}^{[3]}|^2$ and $\bar{\eta}^{[3]}$ for the parametric choice $d = 1, b = 2, \omega_0 = \frac{1}{2}, K_0 = 1, J_0 = 0, J_1 = 100, J_2 = 0$ are plotted in the Figures 19-21. Similarly, there is another kind third-order rogue wave, for example, $|\bar{E}^{[3]}|^2$ is higher than third-rogue above. The dynamical evolution of $|\bar{E}^{[3]}|^2$, $|\bar{p}^{[3]}|^2$ and $\bar{\eta}^{[3]}$ for the parametric choice $d = \frac{4}{3}, b = 0, \omega_0 = \frac{1}{2}, K_0 = 1, J_0 = 0, J_1 = 0, J_2 = 0$ are plotted in the Figures 22-24. Note that eigenvalue $\lambda_1 = \lambda_3 = \lambda_5$ is real. The eigenvalue of rogue waves are different from the eigenvalue of solutions given in the past. According to analysis above, the n -order rogue waves may be controlled by $n + 3$ free parameters.

From the above discussions, it is interesting to point out that the down amplitudes are dominant in the profile of rogue waves $\tilde{p}^{[1]}$ and $\tilde{\eta}^{[1]}$, so they are new kind of rogue waves when compared with the typical bright rogue wave $\tilde{E}^{[1]}$, which are corresponding to the dark breathers in Figure 2 and Figure 3. So from our earlier understanding of breathers in other physical systems, we call these new type of solutions as dark rogue waves. Moreover, the dark rogue wave $\tilde{p}^{[1]}$ has one upper ring and three down peaks, and dark rogue wave $\tilde{\eta}^{[1]}$ has two lumps and one down peak. According to analysis, the n -order rogue waves must be generated by n -order breather solution.

From the detailed literature on rogue waves, to the best of our knowledge, so far only bright rogue waves have been analyzed in detail but there is little report about the dark rogue waves in physical system. In the case of bright optical rogue waves, many results have actually connected the generation of supercontinuum generation (SCG) with rogue waves [57]. In recent years, the supercontinuum white coherent source has attracted a lot of attention because of its potential applications in optical coherence tomography, spectroscopy, wavelength division multiplexing, etc. As reported in ref. [58], the modulational instability (MI) conditions for the generation of ultra-short pulses has already been investigated in the erbium doped nonlinear fibre and occurrences of nonconventional side bands have also been observed. This type of nonconventional side bands will be very useful to generate large MI bandwidth which intern generates very short pulses. In this way, we believe that our rogue wave results in this paper can also be connected to the generation of SCG. Similarly, the occurrence of dark rogue wave can also be connected to the results of ref. [58], in the following manner: In our above work [58], it has been shown that both bright and dark SIT solitons can be generated in the case of the anomalous and normal group velocity dispersion (GVD), in contrast to the well-established results in the conventional fibre, where bright and dark solitons exists in the anomalous and normal GVD regions, respectively. From the above results, it is clear that the formation of dark rogue waves can also be connected in a similar way. Thus, it is interesting to analyze the relation connecting the MI, SCG and rogue wave formation in optical system.

4. CONCLUSION

Thus, in this article, we have reported the rogue waves of the three physical fields E , p , and η in a resonant erbium-doped fibre system, which is governed by the NLS-MB equations. These rogue waves are constructed by a Taylor series expansion of the corresponding breather solutions of the NLS-MB equations. As expected, in contrast to the usual bright rogue wave E , we observe dark rogue waves for p and η . The main feature of the dark rogue waves is the appearance of two (or more) dominant down peaks in its profile. In particular, there is one upper ring in the profile of the p , so it may be called as dark ring-rogue wave. The explicit form of $\bar{E}^{[n]}$, $\bar{p}^{[n]}$ and $\bar{\eta}^{[n]}$ are given by the determinant representation of the n-fold DT. The rogue waves in previous section can also be connected to the supercontinuum generation.

As we have already described in the introduction, the singularity [13] of the solutions generated by the DT is the main constraint to generate the dark rogue waves of the defocusing NLS equation. This perhaps shows that the dark rogue wave of the defocusing NLS equation can be investigated by other way such as by means of Hirota method. From the determinant representation of the T_n , it is interesting to generate the higher order rogue waves so that the dynamical interactions of rogue waves can be analysed. Moreover, it is also possible to obtain new type of rogue waves for other important coupled system in optics [59], such as the CH-MB equations.

Acknowledgments This work is supported by the NSF of China under Grant No.10971109 and K.C.Wong Magna Fund in Ningbo University. Jingsong He is also supported by Program for NCET under Grant No.NCET-08-0515. We thank Prof. Yishen Li(USTC, Hefei, China) for his useful suggestions on the rogue wave. KP wishes to thank the DST, DAE-BRNS, UGC, CSIR, Government of India, for the financial support through major projects.

REFERENCES

- [1] A.Hasegawa and F.Tappert, 1973, Transmission of stationary nonlinear optical pulses in dispersive dielectric fibers.I.Anomalous dispersion, *Appl.Phys.Lett.* 23, 142-144.
- [2] S.L.McCall and E.L.Hahn, 1967, Self-Induced Transparency by Pulsed Coherent Light, *Phys.Rev.Lett.* 18, 908-911.
- [3] A.I. Maimistov and E. A. Manykin, 1983, The propagation of ultrashort optical pulses in nonlinear resonance light guides, *Sov. Phys. JETP.* 85, 1177-1181.
- [4] K. Porsezian and K. Nakkeeran, 1995, Optical soliton propagation in a coupled system of the nonlinear Schrodinger equation and the Maxwell-Bloch equations, *J. Mod. Opt.* 42, 1953-1958.
- [5] S. Kakei and J. Satsuma, 1994, Multi-Soliton Solutions of a Coupled System of the Nonlinear Schrödinger Equation and the Maxwell-Bloch Equations, *J. Phys. Soc. Japan* 63, 885-894.
- [6] M. Nakazawa, E. Yamada and H. Kubota, 1991, Coexistence of self-induced transparency soliton and nonlinear Schrödinger soliton, *Phys. Rev. Lett.* 66, 2625-2628.
- [7] M. Nakazawa, E. Yamada and H. Kubota, 1991, Coexistence of a self-induced-transparency soliton and a nonlinear Schrödinger soliton in an erbium-doped fiber, *Phys. Rev. A.* 44, 5973-5987.
- [8] K. Porsezian and K.Nakkeeran, 1995, Optical Soliton Propagation in an Erbium Doped Nonlinear Light Guide with Higher Order Dispersion, *Phys. Rev. Lett.* 74, 2941-2944.
- [9] K. Porsezian a, P. Seenivasakumaran, and R. Ganapathy, 2006, Optical solitons in some deformed MB and NLS-MB equations, *Phys. Lett. A.* 348, 233-243.
- [10] A.Mahalingam, K.Porsezian, M.S.Mani Rajan, and A.Uthayakumar, 2009, Propagation of dispersion-nonlinearity-managed solitons in an inhomogeneous erbium-doped fiber system, *J. Phys. A: Math. Theor.* 42, 165101 (12pp).
- [11] C. G. Latchio Tiofack, Alidou. Mohamadou, Timoleon C Kofane and K. Porsezian, 2010, Exact quasi-soliton solutions and soliton interaction for the inhomogeneous coupled Hirota-Maxwell-Bloch equations, *J. Opt.* 12, 085202 (9pp).
- [12] J.S.He, Y.Cheng and Y.S.Li, 2002, The Darboux Transformation for NLS-MB Equations, *Commun. Theor. Phys.* 38, 493-496.
- [13] G.Neugebauer and R.Meinel, 1984, General N-soliton solution of the AKNS class on arbitrary background, *Phys.Lett.A.* 100, 467-470.
- [14] V. B. Matveev and M.A. Salle, 1991, *Darboux Transformations and Solitons* (Springer-Verlag, Berlin).
- [15] C.Kharif and E.Pelinovsky, 2003, Physical mechanisms of the rogue wave phenomenon, *Eur.J.Mech.B (Fluids)*. 22, 603-634.
- [16] C.Kharif, E.Pelinovsky and A.Slunyaev, 2009, *Rogue Waves in the Ocean* (Berlin: Springer).

- [17] A.Chabchoub, N.P.Hoffmann and N.Akhmediev, 2011, Rogue Wave Observation in a Water Wave Tank, *Phys. Rev. Lett.* 106,204502 (4pp).
- [18] I.Didenkulova1 and E.Pelinovsky, 2011, Rogue waves in nonlinear hyperbolic systems (shallow-water framework), *Nonlinearity.* 24, R1-R18.
- [19] D. H. Peregrine, 1983, Water waves, Nonlinear Schrödinger equations and their solutions, *J. Aust. Math. Soc. Ser. B, Appl. Math.* 25, 16-43.
- [20] Kristian, B.Dysthe and K.Trulsen, 1999, Note on Breather Type Solutions of the NLS as Models for Freak-Waves, *Phys Scri. 82*, 48-52.
- [21] V.E.Zakharov and L.A.Ostrovsky, 2009, Modulation instability: the beginning, *Phys.D.* 238, 540 (8pp).
- [22] N.N.Akhmediev and V.I.Korneev, 1986, Modulation instability and periodic solutions of the Nonlinear Schrödinger equation, *Theor. Math. Phys.* 69, 1080-1093.
- [23] I.Shrira and V.Geogjaev, 2010, What makes the Peregrine soliton so special as a prototype of freak waves?, *J.Eng.Math.* 67, 11-22.
- [24] Zhenya.Yan, 2009, Nonautonomous "rogons" in the inhomogeneous nonlinear Schrödinger equation with variable coefficients, *Phys. Lett.A.* 374, 672-679.
- [25] ChaoQing Dai, GuoQuan Zhou and JieFang Zhang, 2012, Controllable optical rogue waves in the femtosecond regime, *Phys. Rev. E.* 85, 016603(7pp).
- [26] L.H.Ying,Z.Zhuang,E. J.Heller and L.Kaplan, 2011, Linear and nonlinear rogue wave statistics in the presence of random currents, *Nonlinearity.* 24, R67-R87.
- [27] P. Dubard, P. Gaillard, C. Klein, V.B. Matveev, 2010, On multi-rogue wave solutions of the NLS equation and positon solutions of the KdV equation, *Eur. Phys. J. Special Topics* 185, 247-258.
- [28] P. Dubard, V.B. Matveev, 2011, Multi-rogue waves solutions to the focusing NLS equation and the KP-I equation, *Nat. Hazards. Earth. Syst. Sci.* 11, 667-672.
- [29] P. Gaillard, 2011, Families of quasi-rational solutions of the NLS equation and multi-rogue waves, *J. Phys. A: Math. Theor.* 44, 435204 (15pp).
- [30] Boling.Guo,Liming.Ling and Q.P.Liu, 2012, Nonlinear Schrödinger Equation: Generalized Darboux Transformation and Rogue Wave Solutions, *Phys. Rev. E.* 85, 026607(9pp).
- [31] Yasuhiro. Ohta, Jianke. Yang, 2011, General high-order rogue waves and their dynamics in the nonlinear Schrödinger equation, *Proc. R. Soc. A.* (doi:10.1098/rspa.2011.0640)(25pp).
- [32] N. Akhmediev,J. M. Soto-Crespo and A. Ankiewicz, 2009, How to excite a rogue wave, *Phys. Rev. A.* 80, 043818 (7pp).
- [33] J. S. He, H. R. Zhang, L. H. Wang, K. Porsezian and A. S. Fokas, 2012, A generating mechanism for higher order rogue waves, *arXiv:1209.3742v2.*
- [34] V. Fedun, M.S.Ruderman and R. Erdélyi, 2008, Generation of short-lived large-amplitude magnetohydrodynamic pulses by dispersive focusing, *Phys. Lett.A.* 372, 6107-6110.
- [35] M.S. Ruderman, 2010, Freak waves in laboratory and space plasmas, *Euro. Phys. Jour.* 185, 57-66.
- [36] Shuwei. Xu, Jingsong.He and Lihong.Wang, 2011, The Darboux transformation of the derivative nonlinear Schrodinger equation, *J. Phys. A: Math. Theor.* 44, 305203 (22pp).
- [37] Shuwei. Xu, Jingsong.He and Lihong.Wang, 2012, Two kinds of rogue waves of the general nonlinear Schrödinger equation with derivative, *Europhys. Letter.* 97, 30007 (6pp).
- [38] W.M.Moslem, P.K.Shukla and B.Eliasson, 2011, Surface plasma rogue waves, *Euro.Phys.Lett.* 96, 25002 (5pp).
- [39] Boling Guo, Liming Ling and Q. P. Liu, 2012, High-Order Solutions and Generalized Darboux Transformations of Derivative Nonlinear Schrödinger Equations, *Stud. Appl. Math.* DOI: 10.1111/j.1467-9590.2012.00568.x.
- [40] D. R. Solli, C. Ropers, P. Koonath, and B. Jalali, 2007, Optical rogue waves, *Nature*, 450, 1054-1057.
- [41] B. Kibler, J. Fatome, C. Finot, G. Millot,F. Dias, G. Genty,N. Akhmediev and J. M. Dudley, 2010, The Peregrine soliton in nonlinear fibre optics, *Nature.Physics.* 6, 790-795.
- [42] F. T. Arecchi, U. Bortolozzo,A. Montina and S. Residori, 2011, Granularity and Inhomogeneity Are the Joint Generators of Optical RogueWaves, *Phys. Rev. Lett.* 106, 153901 (4pp).
- [43] A.Ankiewicz, J. M. Soto-Crespo and N. Akhmediev, 2010, Rogue waves and rational solutions of the Hirota equation, *Phys. Rev. E.* 81, 046602 (8pp).
- [44] Guangye Yang, Lu Li and Suotang Jia, 2012, Peregrine rogue waves induced by the interaction between a continuous wave and a soliton, *Phys. Rev. E.* 85, 046608(8pp).
- [45] Yongsheng Tao and Jingsong He, 2012, Multisolitons, breathers, and rogue waves for the Hirota equation generated by the Darboux transformation, *Phys. Rev. E* 85, 026601 (7pp).
- [46] A.Ankiewicz, N.Akhmediev and J. M. Soto-Crespo, 2010, Discrete rogue waves of the Ablowitz-Ladik and Hirota equations, *Phys. Rev. E.* 82, 026602 (7pp).
- [47] Boling.Guo and Liming.Ling, 2011, Rogue Wave, Breathers and Bright-Dark-Rogue Solutions for the Coupled Schrödinger Equations. *Chin. Phys. Lett.* 28, 110202 (1-4).

[48] Fabio Baronio, Antonio Degasperis, Matteo Conforti and Stefan Wabnitz, 2012, Solutions of the Vector Nonlinear Schrödinger Equations: Evidence for Deterministic Rogue Waves, *Phys. Rev. Lett.* 109, 044102(4pp).

[49] BaoGuo.Zhai, WeiGuo. Zhang, XiaoLiWang and HaiQiang Zhang, 2012, Multi-rogue waves and rational solutions of the coupled nonlinear Schrödinger equations, *Nonlinear Anal. RWA*. doi:10.1016/j.nonrwa.2012.04.010.

[50] Zhenyun Qin and Gui Mu, 2012, Matter rogue waves in an $F = 1$ spinor Bose-Einstein condensate, *Phys. Rev. E*. 86, 036601(7pp).

[51] Rider. Jaimes-Reátegui, Ricardo. Sevilla-Escoboza and G.Huerta-Cuellar, 2011, Rogue Waves in a Multistable System, *Phys. Rev. Lett.* 107, 274101 (5pp).

[52] V.E.Zakharov and A.B.Shabat, 1973, Interaction between solitons in a stable medium, *Soviet.Phys.JETP*.37, 823-828.

[53] Jingsong. He, Shuwei. Xu and K. Porsezian, 2012, New Types of Rogue Wave in an Erbium-Doped Fibre System. *J. Phys. Soc. Jpn.* 81, 033002 (4pp).

[54] J.S.He, L.Zhang, Y.Cheng and Y.S.Li, 2006, Determinant representation of Darboux transformation for the AKNS system, *Science in China Series A: Mathematics*.12, 1867-1878.

[55] A. Ankiewicz, J.D. Kedziora, N. Akhmediev, 2011, rogue wave triplets, *Phys. Lett.A*. 375, 2782-2785.

[56] David.J. Kedziora, Adrian. Ankiewicz, and Nail. Akhmediev, 2011, Circular rogue wave clusters, *Phys. Rev. E*. 84, 056611 (7pp).

[57] J.M.Dudley and J.R.Taylor (Eds.), 2010, *Supercontinuum Generation in Optical fibres*(Cambridge,Cambridge University Press).

[58] B .Kalithasan, K.Porsezian, P.T.Dinda and B .A.Malomed, 2009, Modulational Instability and Generation of Self-Induced Transparency Solitons in Resonant Optical Fiber, *J. Optics A: Pure and Applied Optics* 11, 045205.

[59] Chuanzhong Li, Jingsong He and K. Porsezian, 2012, Rogue waves of the Hirota and the Maxwell-Bloch equations, *arXiv:1205.1191v1*.

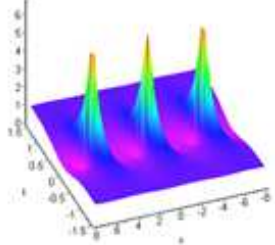


FIGURE 1. The first order breather $|E^{[1]}|^2$ given with specific parameters $d = 1, b = 2, \omega_0 = \frac{1}{2}, \alpha_1 = \frac{4}{5}$. There are one upper peak and two caves in each periodic unit.

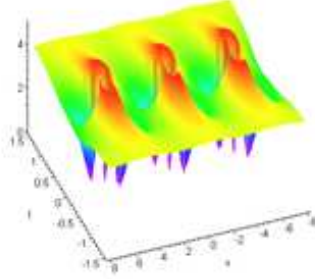


FIGURE 2. The first order dark breather $|p^{[1]}|^2$ for the values used in Figure 1. There are a upper ring and three down peaks in each periodic unit.

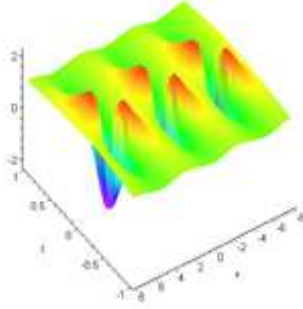


FIGURE 3. The first order dark breather $\eta^{[1]}$ for the values used in Figure 1. There are two lumps and one down peak in each periodic unit.

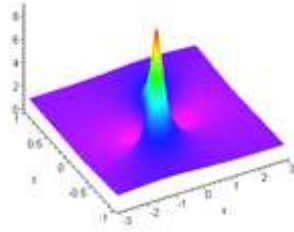


FIGURE 4. The first order rogue wave $|\tilde{E}^{[1]}|^2$ with specific parameters $d = 1, b = 2, \omega_0 = \frac{1}{2}$. There are one upper peak and two caves.

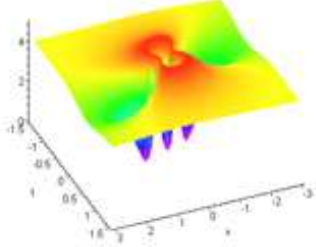


FIGURE 5. The first order dark rogue wave $|\tilde{p}^{[1]}|^2$ for the values used in Figure 4. There are one upper ring and three down peaks.

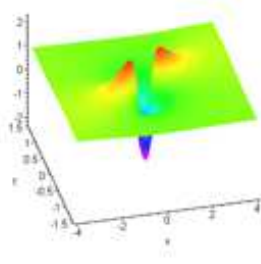


FIGURE 6. The first order dark rogue wave $\tilde{\eta}^{[1]}$ for the values used in Figure 4. There are two lumps and one down peak.

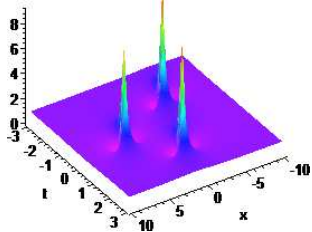


FIGURE 7. The second order rogue wave $|\tilde{E}^{[2]}|^2$ given by eq.(28) with specific parameters $d = 1, b = 2, \omega_0 = \frac{1}{2}, K_0 = 1, J_0 = 0, J_1 = 100$.

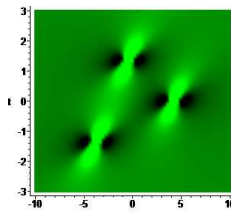


FIGURE 8. Contour plot of the wave amplitudes of $|\tilde{E}^{[2]}|^2$ for the values used in Figure 7.

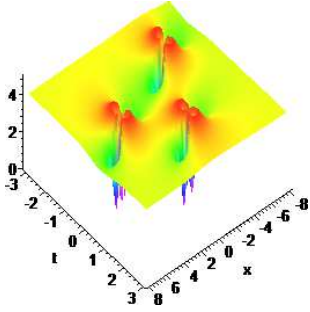


FIGURE 9. The second order dark rogue wave $|\bar{p}^{[2]}|^2$ given by eq.(29) for the values used in Figure 7.

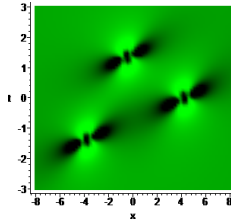


FIGURE 10. Contour plot of the wave amplitudes of $|\bar{p}^{[2]}|^2$ for the values used in Figure 7.

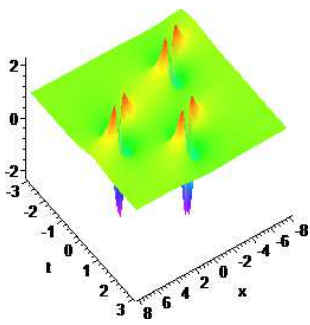


FIGURE 11. The second order dark rogue wave $\bar{\eta}^{[2]}$ given by eq.(30) for the values used in Figure 7.

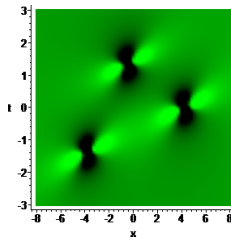


FIGURE 12. Contour plot of the wave amplitudes of $\bar{\eta}^{[2]}$ for the values used in Figure 7.

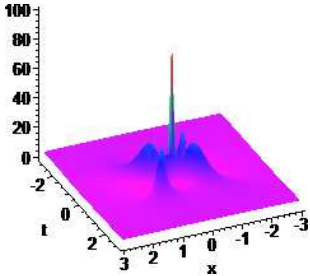


FIGURE 13. The second order rogue wave $|\bar{E}^{[2]}|^2$ given by eq.(28) with specific parameters $d = 2, b = 0, \omega_0 = \frac{1}{2}, K_0 = 1, J_0 = 0, J_1 = 0$.

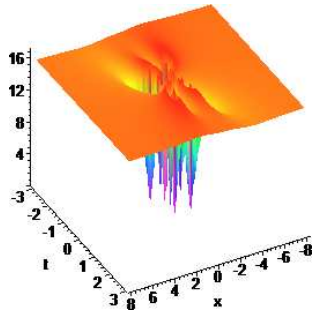


FIGURE 14. The second order dark rogue wave $|\bar{p}^{[2]}|^2$ given by eq.(29) for the values used in Figure 13.

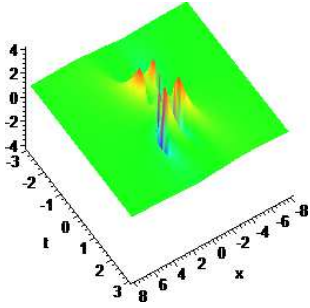


FIGURE 15. The second order dark rogue wave $\bar{\eta}^{[2]}$ given by eq.(30) for the values used in Figure 13.

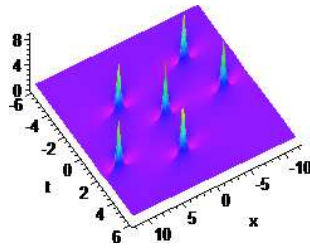


FIGURE 16. The third order rogue wave $|\bar{E}^{[3]}|^2$ given by eq.(28) with specific parameters $d = 1, b = 2, \omega_0 = \frac{1}{2}, K_0 = 1, J_0 = 0, J_1 = 0, J_2 = 8000$.

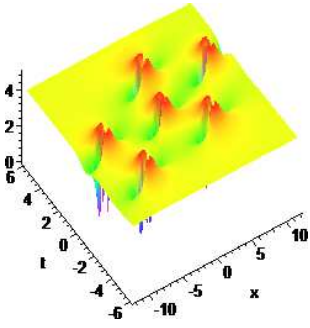


FIGURE 17. The third order dark rogue wave $|\bar{p}^{[3]}|^2$ given by eq.(29) for the values used in Figure 16.

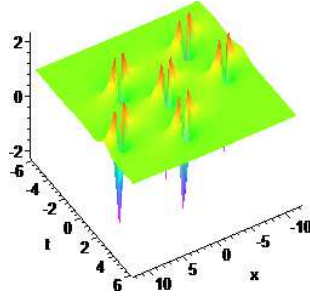


FIGURE 18. The third order dark rogue wave $\bar{\eta}^{[3]}$ given by eq.(30) for the values used in Figure 16.

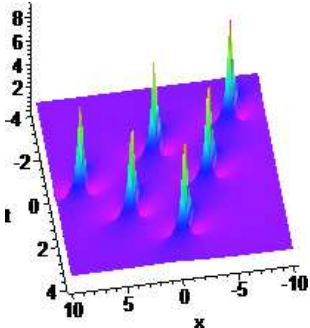


FIGURE 19. The third order rogue wave $|\bar{E}^{[3]}|^2$ given by eq.(28) with specific parameters $d = 1, b = 2, \omega_0 = \frac{1}{2}, K_0 = 1, J_0 = 0, J_1 = 100, J_2 = 0$.

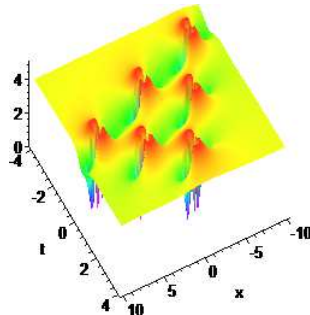


FIGURE 20. The third order dark rogue wave $|\bar{p}^{[3]}|^2$ given by eq.(29) for the values used in Figure 19.

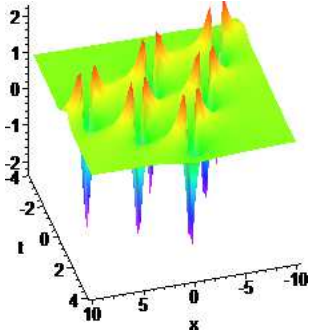


FIGURE 21. The third order dark rogue wave $\bar{\eta}^{[3]}$ given by eq.(30) for the values used in Figure 19.

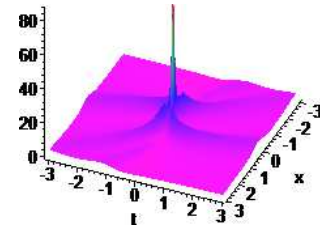


FIGURE 22. The third order rogue wave $|\bar{E}^{[3]}|^2$ given by eq.(28) with specific parameters $d = \frac{4}{3}, b = 0, \omega_0 = \frac{1}{2}, K_0 = 1, J_0 = 0, J_1 = 0, J_2 = 0$.

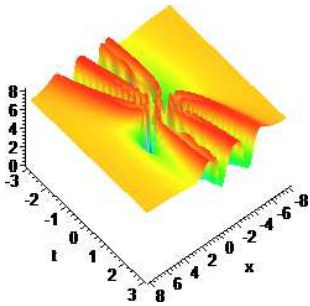


FIGURE 23. The third order dark rogue wave $|\bar{p}^{[3]}|^2$ given by eq.(29) for the values used in Figure 22.

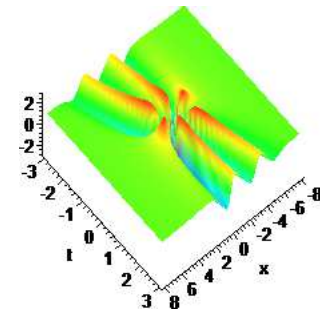


FIGURE 24. The third order dark rogue wave $\bar{\eta}^{[3]}$ given by eq.(30) for the values used in Figure 22.